Phys. Lett. B 876 (2026) 140411

Contents lists available at ScienceDirect

Physics Letters B

journal homepage: www.elsevier.com/locate/physletb

Letter

The heavy quark-antiquark asymmetry in the variable flavor number scheme

A. Behring [a], J. Blümlein [b,c,*], A. De Freitas [d], A. von Manteuffel [e], C. Schneider [d], K. Schönwald [f]

[a] Max-Planck-Institut für Physik, Boltzmannstraße 8, Garching, 85748, Germany
[b] Deutsches Elektronen-Synchrotron DESY, Platanenallee 6, Zeuthen, 15738, Germany
[c] Institut für Theoretische Physik III, IV, TU Dortmund, Otto-Hahn Straße 4, Dortmund, 44227, Germany
[d] Research Institute for Symbolic Computation (RISC), Johannes Kepler University, Altenberger Straße 69, Linz, A-4040, Austria
[e] Institut für Theoretische Physik, Universität Regensburg, Regensburg, 93040, Germany
[f] Theoretical Physics Department, CERN, CH-1211, Geneva 23, Switzerland

ARTICLE INFO

Editor: Feng Bo

Keywords:
Parton distribution
Mass effects
Anomalous dimensions
Massive operator matrix elements in QCD

ABSTRACT

The twist-2 heavy-quark and antiquark distributions, as defined in the variable flavor number scheme, turn out to be different due to QCD corrections from three-loop onward. This is caused by terms containing the color factor $d_{abc}d^{abc}$ in the heavy-flavor massive pure-singlet operator matrix elements (OMEs) $A_{Qq}^{\mathrm{PS},s,(3)}$ for odd moments in the unpolarized case and for $\Delta A_{Qq}^{\mathrm{PS},s,(3)}$ for even moments in the polarized case. The dependence on the factorization scale of the OMEs is ruled by the anomalous dimensions $\gamma_{qq}^{\mathrm{NS},s,(2)}$ and $\Delta\gamma_{qq}^{\mathrm{NS},s,(2)}$. The polarized calculations are performed in the Larin scheme. We compute the corresponding three-loop heavy-flavor distributions $(\Delta)f_Q(x,Q^2) - (\Delta)f_{\overline{Q}}(x,Q^2)$. Compared to the sum of the heavy-quark and antiquark parton distributions, their difference is small, however, non-vanishing.

1. Introduction

Parton distributions rule a wide range of elementary particle phenomenology, and their precise knowledge is instrumental for the study of many scattering processes Refs. [1,2]. In this context, a central question concerns the composition of the nucleons in terms of sea quarks and whether there are differences between the sea quark and antiquark distributions.

The light-flavor quark and antiquark distribution functions of the nucleons $u(x,Q^2)$, $d(x,Q^2)$, $s(x,Q^2)$, $\overline{u}(x,Q^2)$, $\overline{d}(x,Q^2)$, $\overline{s}(x,Q^2)$ are of non-perturbative origin. Their first moments

$$I_q = \int_0^1 dx[q(x,Q^2) - \overline{q}(x,Q^2)] \tag{1}$$

obey the sum rules

$$I_u = 2, \quad I_d = 1, \quad I_s = 0 \tag{2}$$

for unpolarized protons. The sum rule for the strange quarks applies also to other higher mass pure sea quark species. Here x denotes the Bjorken variable, and $Q^2 = -q^2$ the virtuality in the deep-inelastic scattering process. In the polarized case, one has [3][1]

$$I_{\Delta u} = 0.928 \pm 0.014, \quad I_{\Delta d} = -0.342 \pm 0.018, \tag{3}$$

see also Refs. [4–6]. These constants are related to the hyperon β-decay parameters, cf. Refs. [7,8]. While the up- and down-quark and antiquark distributions are different, and there is no $SU_F(3)$ sea quark symmetry [9,10], it has been discussed in Refs. [11–23] that there is also a strange quark-antiquark difference. In Ref. [20], massless evolution effects from a starting scale Q_0^2 to a virtuality Q^2 were studied for strange, charm and bottom, concerning the creation of an asymmetry between quark and antiquark distributions, although, without considering mass effects. In Ref. [14], also a possible charm-anticharm difference in the intrinsic charm model [24,25] was discussed. In the following, we consider only the so-called 'extrinsic' contributions, which are calculated perturbatively in Quantum Chromodynamics (QCD) to three-loop order.

Parton distributions at any twist [26] are no observables beyond lowest order in QCD [27–31]. As also the case for couplings and masses, one defines étalons in suitable schemes, as, e.g., the $\overline{\mathrm{MS}}$ scheme [32] or the

[1] Here and in the following Δ marks quantities in the polarized case.

* Corresponding author.
E-mail address: Johannes.Bluemlein@desy.de (J. Blümlein).

https://doi.org/10.1016/j.physletb.2026.140411
Received 15 December 2025; Received in revised form 27 March 2026; Accepted 30 March 2026
Available online 1 April 2026

Larin scheme [33], to allow for comparisons. This also applies to the unpolarized and polarized twist-2 parton densities.

The fixed flavor number scheme is based on describing the nucleon substructure by three massless parton distributions and the gluon distribution at the level of twist-2 in deep-inelastic scattering. Heavy-quark corrections emerge as inclusive perturbative contributions from $O(a_s)$ onward, with $a_s = \alpha_s/(4\pi) = g_s^2/(16\pi^2)$ the strong coupling constant, both in terms of real and virtual corrections. At very large virtualities $Q^2 \gg m_Q^2$, with m_Q the heavy-quark mass, one may describe the heavy-flavor corrections to deep-inelastic scattering (DIS) in the variable flavor number scheme (VFNS) outlined in Ref. [34], by redefining the parton distributions. [2]

They now receive process-independent heavy-flavor corrections due to massive operator matrix elements. This is necessary to describe the massive Wilson coefficients in the asymptotic region $Q^2 \gg m_Q^2$ correctly, which is not possible in a pure massless approach. In this way, one also introduces the heavy-flavor parton distributions.

In the present paper, we calculate the heavy quark-antiquark asymmetry in the parton distributions within the VFNS by exploiting computer algebra methods. Flavor contributions of this kind do not contribute to the well measured unpolarized and polarized structure functions $F_2(x,Q^2)$ and $g_1(x,Q^2)$, for which we derived the single-mass VFNS to three-loop order in Ref. [39]. In the neutral current case,[3] which we will consider in the following, heavy quark-antiquark difference terms emerge in the γZ-interference and ZZ structure functions $xF_3^{J_1,J_2}(x,Q^2)$ and $g_5^{J_1,J_2}(x,Q^2)$, with $J_k \in \{\gamma, Z\}$, cf. Ref. [42].[4]

The paper is organized as follows. In Section 2, we describe the basic formalism. The unpolarized and polarized heavy quark-antiquark distribution asymmetries are calculated perturbatively in Section 3. Their logarithmic contributions due to the factorization scale are ruled by the anomalous dimensions $(\Delta)\gamma_{qq}^{\rm NS,s,(2)}$, cf. [43–46]. We have newly computed $\Delta\gamma_{qq}^{\rm NS,s,(2)}$ by using different methods. In Section 4, we illustrate the flavor asymmetry for charm and bottom and compare to the sum of both distributions. Section 5 contains the conclusions. We attach ancillary files of the OMEs in Mellin-N and x-space, as well as a `Fortran` code for their numerical evaluation.

2. Basic formalism

In the following we will work in Mellin-N space, using the transformation

$$\mathbf{M}[f(x)](N) = \int_0^1 dx\, x^{N-1} f(x) \tag{4}$$

for the functions $f(x)$ given in momentum fraction x-space. In the single-mass VFNS [34,39], the sum and difference of the heavy-quark contributions are given by the following relations

$$\begin{aligned}(\Delta)f_{Q+\overline{Q}} &\equiv (\Delta)f_Q(N,Q^2,N_F+1) + (\Delta)f_{\overline{Q}}(N,Q^2,N_F+1)\\ &= (\Delta)A_{Qq}^{\rm PS}\cdot(\Delta)\Sigma^+(N,Q^2,N_F) + (\Delta)A_{Qg}\cdot(\Delta)G(N,Q^2,N_F),\end{aligned} \tag{5}$$

$$\begin{aligned}(\Delta)f_{Q-\overline{Q}} &\equiv (\Delta)f_Q(N,Q^2,N_F+1) - (\Delta)f_{\overline{Q}}(N,Q^2,N_F+1)\\ &= (\Delta)A_{Qq}^{\rm PS,s}\cdot(\Delta)\Sigma^-(N,Q^2,N_F).\end{aligned} \tag{6}$$

The massive OMEs $(\Delta)A_{Qq}^{\rm PS}$ and $(\Delta)A_{Qg}$ were computed to three-loop order in Refs. [47–50]. The flavor combination in Eq. (5) contributes to the heavy-flavor corrections to the structure functions F_2 and g_1, respectively. The OMEs $(\Delta)A_{Qq}^{\rm PS,s,(3)}$ are calculated in the present paper. For the quark contributions, the heavy-quark distributions are driven by the distributions

$$(\Delta)\Sigma^\pm = [(\Delta)u \pm (\Delta)\overline{u}] + [(\Delta)d \pm (\Delta)\overline{d}] + [(\Delta)s \pm (\Delta)\overline{s}], \tag{7}$$

and for the sum, also by the gluon distributions $(\Delta)G$. The emergence of the color factor $d_{abc}d^{abc}$ in $(\Delta)A_{Qq}^{\rm PS,s,(3)}(N)$ is caused by the diagrammatic topology of $(\Delta)A_{Qq}^{\rm PS,(3)}(N)$ in the single-mass case, cf. Refs. [47,48], taking the odd moments for $A_{Qq}^{\rm PS,(3)}$ and the even moments for $\Delta A_{Qq}^{\rm PS,(3)}$. In the pure-singlet case, the external lines are (directed) massless fermions. One could, as well, consider the OME $(\Delta)A_{Qg}^{(3)}(N)$ with the same choice of moments. We checked that individual diagrams contain $d_{abc}d^{abc}$ terms, but they add up to zero due to the fact that gluon propagators have no direction. Therefore, there is no gluonic term in Eq. (6). The color factor $d_{abc}d^{abc}$ is given by $d_{abc}d^{abc} = (N_c^2-1)(N_c^2-4)/N_c = 40/3$ and $N_c = 3$ in the case of QCD.[5]

There are also two other non-singlet distributions, $(\Delta)D_{3,(8)}(N,Q^2)$,

$$(\Delta)D_3^\pm = \Delta(u \pm \overline{u}) - \Delta(d \pm \overline{d}), \tag{8}$$

$$(\Delta)D_8^\pm = \Delta(u \pm \overline{u}) + \Delta(d \pm \overline{d}) - 2\Delta(s \pm \overline{s}). \tag{9}$$

By decoupling of a heavy-quark Q in the VFNS, the distributions $(\Delta)D_{3,8}^\pm$ are modified by

$$(\Delta)D_{3,8}^\pm(N,Q^2,N_F+1) = (\Delta)A_{qq,Q}^{\rm NS}\ \cdot\ (\Delta)D_{3,8}^\pm(N,Q^2,N_F), \tag{10}$$

see Refs. [34,39]. In the unpolarized +(−) cases the even (odd) moments of $A_{qq,Q}^{\rm NS}$ are taken and in the polarized case the odd (even) moments. The OMEs $A_{qq,Q}^{\rm NS}$ were calculated in Ref. [52]. However, they map between massless quark distributions only.

The flavor combinations $(\Delta)f_{Q-\overline{Q}}$ emerge in electroweak structure functions, such as the neutral current unpolarized structure function $xF_3(x,Q^2)$ and polarized structure function $g_5(x,Q^2)$. Their crossing relations, cf. Ref. [42], are in accordance with the respective choice of moments mentioned before. In the unpolarized case, xF_3 can be measured from

$$\begin{aligned}B^-(\lambda) &= \frac{xQ^4}{4\pi\alpha^2 Y_-\kappa_Z(Q^2)}\left[\frac{d\sigma^+(-\lambda)}{dxdQ^2} - \frac{d\sigma^-(+\lambda)}{dxdQ^2}\right]\\ &= (a_e - \lambda v_e)xF_3^{\gamma Z}(x,Q^2)\\ &\quad +\kappa_Z(Q^2)[2v_e a_e + \lambda(v_e^2+a_e^2)]xF_3^{ZZ}(x,Q^2),\end{aligned} \tag{11}$$

cf. Refs. [53–55]. Analogous relations hold in the polarized case. Here $Y_- = 1-(1-y)^2$, $y = P.q/l.q$, P is the proton momentum, l the lepton momentum, and λ denotes the degree of the longitudinal lepton beam polarization. The labels $\pm$ of the cross sections σ refer to the charge of the incoming charged lepton. The weak couplings of the electron are $v_e = -1/2 + 2\sin^2\theta_W, a_e = -1/2$, with θ_W the electroweak mixing angel, and $\kappa_Z(Q^2) = Q^2/(Q^2+M_Z^2)/(4\sin^2\theta_W\cos^2\theta_W)$, where M_Z denotes the Z-boson mass. First experimental results on B^- were measured by BCDMS [56] and later at HERA [57]. Future measurements of this quantity can be carried out in a possible later stage at EIC,[6] which requires also polarized positron measurements [58,59]. The measurement is planned also within the LHeC project [60,61].

Let us now turn to the calculation of the OMEs $(\Delta)\hat{A}_{Qq}^{\rm PS,s,(3)}(N)$ under the above choice of moments. The unrenormalized massive on-shell OMEs read

$$\begin{aligned}(\Delta)\hat{A}_{Qq}^{\rm PS,s,(3)}(N)\Big|_{d_{abc}d^{abc}} &= a_s^3\left(\frac{m_Q^2}{\mu^2}\right)^{3\varepsilon/2}\Big[\frac{1}{3\varepsilon}(\Delta)\hat{\gamma}_{qq}^{\rm NS,s,(2)}(N)\\ &\quad +(\Delta)a_{Qq}^{\rm PS,s,(3)}(N)\Big] + O(\varepsilon),\end{aligned} \tag{12}$$

with μ the factorization scale and $\hat{f}(N_F) = f(N_F+1) - f(N_F)$, see also the conventions in the regular pure-singlet case $(\Delta)A_{Qq}^{\rm PS}$ in Refs. [47,48].

[2] Other variants of the VFNS have been discussed in Refs. [35–38], but not yet to three-loop order.

[3] The OMEs in the charged current case are different, as they also contain flavor excitation contributions, cf. Refs. [40,41].

[4] One also could consider the structure function g_4, being related to g_5, cf. Ref. [42].

[5] For different conventions used in the literature, see, however, Ref. [51], Eq. (381), for remarks.

[6] We thank E. Aschenauer and W. Melnitchouk for remarks.

Here the dimensional parameter is defined by $\varepsilon = D - 4$, with D the space-time dimension.

Because these OMEs start at $O(a_s^3)$, the only renormalization concerns the local operator insertion

$$(\Delta)A_{Qq}^{\mathrm{PS,s,(3)}}(N) = Z_{qq}^{-1,\mathrm{PS,s}}(\Delta)\hat{A}_{Qq}^{\mathrm{PS,s,(3)}}(N)\Big|_{d_{abc}d^{abc}} \tag{13}$$

with

$$Z_{qq}^{-1,\mathrm{PS,s}} = 1 - a_s^3\frac{1}{3\varepsilon}(\Delta)\hat{\gamma}_{qq}^{\mathrm{NS,s,(2)}}(N). \tag{14}$$

There is no mass nor coupling renormalization, and no collinear subtraction due to massless subsystems is needed, cf. Ref. [62]. The renormalized OME is given by

$$(\Delta)A_{Qq}^{\mathrm{PS,s,(3)}}(N) = a_s^3\left[\frac{1}{2}(\Delta)\hat{\gamma}_{qq}^{\mathrm{NS,s,(2)}}(N)\ln\left(\frac{m_Q^2}{\mu^2}\right) + (\Delta)a_{Qq}^{\mathrm{PS,s,(3)}}(N)\right], \tag{15}$$

where $(\Delta)a_{Qq}^{\mathrm{PS,s,(3)}}$ denotes the constant part of the unrenormalized massive OME. All massive OMEs are solutions of renormalization group equations, see Refs. [34,39], due to which they account for scale evolution effects, which is also evident from their analytic structures in Mellin space, see Ref. [62]. Note that Eq. (15), derived in the VFNS, differs from Eqs. (16, 19) in a massless evolution approach in Ref. [20], especially by the non-logarithmic term $(\Delta)a_{Qq}^{\mathrm{PS,s,(3)}}$, not considered there, and the scale setting. In the present approach, the strange quark distribution is dealt with as a massless quark since $m_s < \Lambda_{\mathrm{QCD}}$, cf. Ref. [63].

3. The massive operator matrix elements

The technical steps of the present calculation are those described in previous papers, see, e.g., Ref. [49]. We use the packages `QGRAF` [64], `Form` [65,66], `color` [67], `Reduze 2` [68,69] for diagram generation, the performance of the Lorentz- and Dirac algebra, color algebra, and the integration-by-parts reduction. The master integrals are calculated in Mellin N–space using different techniques, which are described in Refs. [70,71]. In the present case, only first–order–factorizable recurrences are obtained, which can be solved by summation technologies based on difference ring theory [72–85], encoded in the package `Sigma` [86,87]. The package `HarmonicSums` [88–105] is used to simplify the final expressions in Mellin-N and x-space.

3.1. The operator matrix element $A_{Qq}^{\mathrm{PS,s,(3)}}$

In the unpolarized case, one obtains the anomalous dimension [43,45]

$$\begin{aligned}\gamma_{qq}^{\mathrm{NS,s,(2)}} &= 4\frac{d_{abc}d^{abc}}{N_c}N_F\frac{1}{2}[1-(-1)^N]\Bigg\{\frac{S_1P_{13}}{(N-1)N^4(1+N)^4(2+N)}\\ &+\frac{2P_{14}}{(N-1)N^5(1+N)^5(2+N)} + \Bigg[-\frac{2P_{12}}{(N-1)N^3(1+N)^3(2+N)}\\ &-\frac{4\left(2+N+N^2\right)^2S_1}{(N-1)N^2(1+N)^2(2+N)}\Bigg]S_{-2}\\ &-\frac{\left(2+N+N^2\right)}{N^2(1+N)^2}[S_3-2S_{-3}+4S_{-2,1}]\Bigg\}\end{aligned} \tag{16}$$

and the constant part of the unrenormalized OME in Mellin space

$$\begin{aligned}a_{Qq}^{\mathrm{PS,s,(3)}} =\ &\frac{4}{3}\frac{d_{abc}d^{abc}}{N_c}\frac{1}{2}[1-(-1)^N]\Bigg\{\frac{S_{2,1}P_1}{2N^3(1+N)^3(2+N)}\\ &+\frac{S_1^2P_3}{4(N-1)N^4(1+N)^4(2+N)} + \frac{S_2P_4}{4(N-1)N^4(1+N)^4(2+N)}\\ &-\frac{3\zeta_3P_5}{2(N-1)N^3(1+N)^3(2+N)} + \frac{S_{-3}P_6}{2(N-1)N^3(1+N)^3(2+N)}\\ &+\frac{S_{-2,1}P_7}{(N-1)N^3(1+N)^3(2+N)} + \frac{S_3P_8}{2(N-1)N^3(1+N)^3(2+N)}\\ &+\frac{P_{11}}{(N-1)N^6(1+N)^6(2+N)^2} + \frac{2+N+N^2}{N^2(1+N)^2}\\ &\times\Bigg[\Bigg[\frac{\left(42+11N+11N^2\right)S_3}{2(N-1)(2+N)} + \frac{\left(14-19N-19N^2\right)S_{-2,1}}{(N-1)(2+N)}\\ &-\frac{3\left(10+7N+7N^2\right)\zeta_3}{2(N-1)(2+N)}\Bigg]S_1 + \frac{\left(-18+13N+13N^2\right)S_{-3}S_1}{2(N-1)(2+N)}\\ &-\frac{4S_{-2}S_2}{(N-1)(2+N)} + \frac{3\left(6+N+N^2\right)S_4}{2(N-1)(2+N)} - \frac{1}{2}S_2^2 + \frac{\left(-2-5N-5N^2\right)S_{-2}^2}{(N-1)(2+N)}\\ &-\frac{12S_{-4}}{(N-1)(2+N)} - \frac{3\left(14+N+N^2\right)S_{3,1}}{2(N-1)(2+N)}\\ &-\frac{6\left(-2+3N+3N^2\right)S_{-2,2}}{(N-1)(2+N)} - \frac{6\left(-2+3N+3N^2\right)S_{-3,1}}{(N-1)(2+N)}\\ &+\frac{12\left(-2+3N+3N^2\right)S_{-2,1,1}}{(N-1)(2+N)}\Bigg] + \Bigg[\frac{P_{10}}{4(N-1)N^5(1+N)^5(2+N)^2}\\ &-\frac{(N-1)(2+N)\left(1+2N+2N^2\right)S_2}{2N^3(1+N)^3}\Bigg]S_1 - \frac{\left(2+N+N^2\right)^2S_{-2}S_1^2}{(N-1)N^2(1+N)^2(2+N)}\\ &+\Bigg[-\frac{2S_1P_2}{(N-1)N^3(1+N)^3(2+N)^2}\\ &+\frac{P_9}{2(N-1)N^4(1+N)^4(2+N)^2}\Bigg]S_{-2}\Bigg\},\end{aligned} \tag{17}$$

which is a new result. Here the nested finite harmonic sums are, cf. Refs. [88,89],

$$S_{b,\vec{a}}(N) = \sum_{k=1}^{N}\frac{(\mathrm{sign}(b))^k}{k^{|b|}}S_{\vec{a}}(k), \quad b, a_i \in \mathbb{Z}\backslash\{0\}, S_\emptyset = 1, \tag{18}$$

setting $S_{\vec{a}}(N) \equiv S_{\vec{a}}$. The polynomials P_i are

$$P_1 = -6N^6 - 26N^5 - 38N^4 - 7N^3 + 17N^2 + 8N + 4, \tag{19}$$
$$P_2 = 2N^7 + 11N^6 + 20N^5 + 39N^4 + 48N^3 + 40N^2 + 48N + 16, \tag{20}$$
$$P_3 = -3N^8 - 12N^7 - 16N^6 - 6N^5 - 30N^4 - 64N^3 - 73N^2 - 40N - 12, \tag{21}$$
$$P_4 = -N^8 - 6N^7 - 8N^6 + 20N^5 + 40N^4 + 4N^3 - 109N^2 - 136N - 60, \tag{22}$$
$$P_5 = N^8 - N^7 - 13N^6 - 4N^5 - N^4 - 43N^3 - 67N^2 - 44N - 20, \tag{23}$$
$$P_6 = 6N^8 + 27N^7 + 17N^6 - 28N^5 - 53N^4 - 13N^3 + 36N^2 - 32N - 24, \tag{24}$$
$$P_7 = 6N^8 + 27N^7 + 61N^6 + 24N^5 - N^4 + 31N^3 + 4N^2 + 32N + 8, \tag{25}$$
$$P_8 = 15N^8 + 63N^7 + 89N^6 + 12N^5 - 125N^4 - 163N^3 - 203N^2 - 132N - 68, \tag{26}$$
$$P_9 = -3N^9 - 14N^8 - 28N^7 + 52N^6 + 141N^5 + 22N^4 - 38N^3 + 36N^2 + 72N + 16, \tag{27}$$
$$P_{10} = -11N^{11} - 67N^{10} - 126N^9 + 6N^8 + 297N^7 - 175N^6 - 1582N^5 - 2468N^4 - 2358N^3 - 1492N^2 - 616N - 112, \tag{28}$$
$$P_{11} = 6N^{12} + 44N^{11} + 140N^{10} + 246N^9 + 254N^8 + 85N^7 + 7N^6 + 410N^5 + 873N^4 + 861N^3 + 478N^2 + 156N + 24, \tag{29}$$
$$P_{12} = N^6 + 3N^5 - 8N^4 - 21N^3 - 23N^2 - 12N - 4, \tag{30}$$
$$P_{13} = -3N^8 - 12N^7 - 16N^6 - 6N^5 - 30N^4 - 64N^3 - 73N^2 - 40N - 12, \tag{31}$$
$$P_{14} = N^8 + 4N^7 + 13N^6 + 25N^5 + 57N^4 + 77N^3 + 55N^2 + 20N + 4. \tag{32}$$

The first moment $N = 1$ both of the anomalous dimension $\gamma_{qq}^{\mathrm{NS,s,(2)}}$ and of $A_{Qq}^{\mathrm{PS,(3),s}}(N)$ vanish. The expression in x-space, $a_{Qq}^{\mathrm{PS,s,(3)}}(x)$, is given in an ancillary file to this paper. It can be expressed by harmonic polylogarithms [93] up to weight $\mathsf{w} = 5$,

$$\begin{aligned}\mathrm{H}_{b,\vec{a}}(x) &= \int_0^x dy f_b(y)\mathrm{H}_{\vec{a}}(y), \quad b, a_i \in \{-1,0,1\}, \mathrm{H}_\emptyset = 1,\\ &f_c(x) \in \left\{\frac{1}{1+x}, \frac{1}{x}, \frac{1}{1-x}\right\} \text{ with} \mathrm{H}_{\underbrace{0,\ldots,0}_{k}}(x) := \frac{1}{k!}\ln^k(x).\end{aligned} \tag{33}$$

In the small-x region one obtains

$$a_{qq}^{\mathrm{PS,s,(3)}}(x) \propto \frac{d_{abc}d^{abc}}{3N_c}\Bigg\{-4\left(16+28\zeta_3+13\zeta_5\right) + \left(186-28\zeta_3\right)\zeta_2 - \frac{43}{5}\zeta_2^2$$

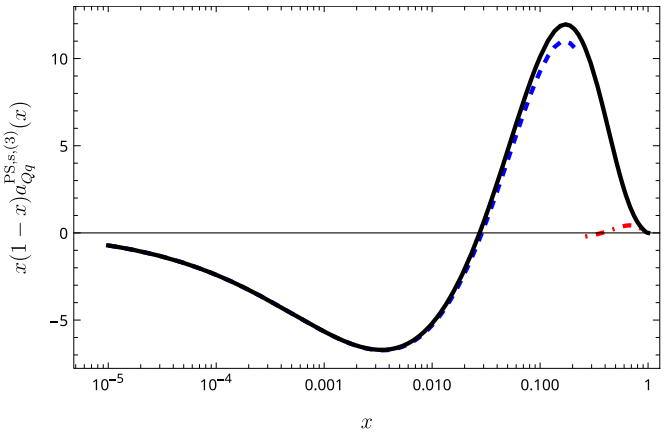

Fig. 1. The constant part of the unrenormalized massive OME $\hat{A}_{Qq}^{\mathrm{PS},s,(3)}$, $a_{Qq}^{\mathrm{PS},s,(3)}$, rescaled by $x(1-x)$. Dashed line: small-x expansion up to the constant term. Dash-dotted line: large-x approximation. Full line: complete result.

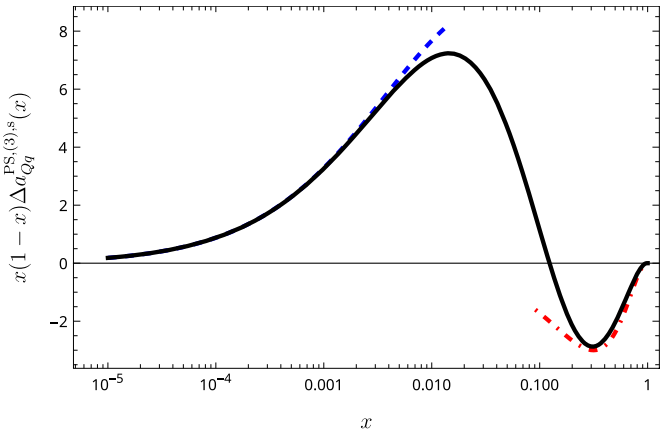

Fig. 2. The constant part of the unrenormalized massive OME $\Delta\hat{A}_{Qq}^{\mathrm{PS},s,(3)}$, $\Delta a_{Qq}^{\mathrm{PS},s,(3)}$, rescaled by $x(1-x)$. Dashed line: small-x expansion up to the constant term. Dash-dotted line: large-x approximation. Full line: complete result.

$$+\left[84-4\zeta_2-42\zeta_2^2+4\zeta_3\right]\ln(x)$$
$$+\left[30+9\zeta_2-28\zeta_3\right]\ln^2(x)+\left[\frac{32}{3}-6\zeta_2\right]\ln^3(x)$$
$$-\frac{1}{2}\ln^4(x)+\frac{1}{5}\ln^5(x)\Bigg\}, \tag{34}$$

and for large x

$$a_{Qq}^{\mathrm{PS},s,(3)}(x)\propto\frac{d_{abc}d^{abc}}{3N_c}(1-x)\Bigg\{-20+13\zeta_2-\frac{21}{5}\zeta_2^2+6\zeta_3$$
$$+\left[17-8\zeta_2-8\zeta_3\right]\ln(1-x)+\left[-3+2\zeta_2\right]\ln^2(1-x)\Bigg\}. \tag{35}$$

In Fig. 1 we illustrate the constant part of the unrenormalized massive OME $\hat{A}_{Qq}^{\mathrm{PS},s,(3)}$, $a_{Qq}^{\mathrm{PS},s,(3)}$, as a function of x. It is remarkable that the small-x expansion, Eq. (34), holds up to relatively large values of x.

3.2. The operator matrix element $\Delta A_{Qq}^{\mathrm{PS},s}$

Since in the contributing diagrams the two insertions of γ_5 are on different fermion lines, we employ the Larin scheme [33] for the calculation of $\Delta A_{Qq}^{\mathrm{PS},s}$. We use three different methods to compute the anomalous dimension $\Delta\gamma_{qq}^{\mathrm{NS},s,(2)}$: *i)* the unrenormalized on-shell OME $\Delta\hat{A}^{\mathrm{PS},s,(3)}$ with massive fermions for even moments, *ii)* the unrenormalized massless off-shell OME $\Delta\hat{A}^{\mathrm{PS},s,(3)}$ for even moments, and *iii)* the forward Compton amplitude for the γZ-interference structure function g_5, see Ref. [42]. Here the projector of Eq. (4.14) in Ref. [106] has been used, which is structurally the same as the one in Eq. (11) of Ref. [107]. We got the same result in all cases,[7]

$$\Delta\gamma_{qq}^{\mathrm{NS},s,(2)}=4\frac{d_{abc}d^{abc}}{N_c}N_F\frac{1}{2}[1+(-1)^N]\Bigg\{\frac{S_1Q_4}{N^4(1+N)^4}$$
$$+\left[-\frac{2\left(1+N+N^2\right)\left(2+N+N^2\right)}{N^3(1+N)^3}-\frac{4(N-1)(2+N)}{N^2(1+N)^2}S_1\right]$$
$$\times S_{-2}-\frac{\left(2+N+N^2\right)}{N^2(1+N)^2}[S_3-2S_{-3}+4S_{-2,1}]\Bigg\}. \tag{36}$$

[7] Our previous calculation used the forward Compton amplitude, erroneously with a different projector for the structure function g_5, Ref. [46], Eqs. (38, 39) and Ref. [44], p. 436. It has now been corrected leading to Eq. (36). After our calculation was finished, we found that in an independent calculation in Ref. [108], using a SCET approach, the same result has been obtained, if one refers to the attachment `dPSLarin.m` there.

The agreement of the results of *i)* and *ii)* shows that potential 'alien' operators, cf., e.g., Ref. [109], play no role in the present case. Additionally, obtaining the anomalous dimension from the forward Compton amplitude requires a different projector than the one used in Refs. [44,46]. At three-loop order the anomalous dimension $\Delta\gamma_{qq}^{\mathrm{NS},s,(2)}$ is scheme invariant. It also obeys the Drell-Yan-Levy rescaling relation in x-space

$$F(x)=-x\mathrm{Re}\left[F\left(\frac{1}{x}\right)\right], \tag{37}$$

see, e.g., Ref. [110], since it appears first at three-loop order.[8] Also the Mellin-inversion of Eq. (16) obeys Eq. (37). The projector given in Ref. [107] was also applied to $\Delta\hat{A}_{Qq}^{\mathrm{PS},(3)}$, i.e. the part $\propto[1-(-1)^N]$, from which the correct polarized three-loop anomalous dimensions $\Delta\gamma_{qq}^{\mathrm{PS},(2)}$ was derived. A corresponding projector, supplemented by a term $\propto p^2$, the off-shellness, needed to remove equation-of-motion terms, Eq. (2.11) of Ref. [46],[9] led to $\Delta\gamma_{qq}^{\mathrm{PS},(2)}$ for the odd moments too.

By method *i)* we also obtain the massive OME, $\Delta\hat{A}_{Qq}^{\mathrm{PS},s,(3)}$, with

$$\Delta a_{Qq}^{\mathrm{PS},s,(3)}(N)=$$
$$\frac{4}{3}\frac{d_{abc}d^{abc}}{N_c}\frac{1}{2}[1+(-1)^N]\Bigg\{\frac{S_{2,1}Q_2}{2N^3(1+N)^3}-\frac{3\zeta_3Q_3}{2N^3(1+N)^2}+\frac{S_1^2Q_4}{4N^4(1+N)^4}$$
$$+\frac{S_2Q_5}{4N^4(1+N)^4}+\frac{S_{-2,1}Q_8}{N^3(1+N)^3}+\frac{S_3Q_9}{2N^3(1+N)^3}$$
$$+\Bigg[\frac{S_2Q_1}{2N^3(1+N)^3}+\frac{Q_{10}}{2N^5(1+N)^5}-\frac{\left(42-11N-11N^2\right)S_3}{2N^2(1+N)^2}$$
$$+\frac{\left(-14-19N-19N^2\right)S_{-2,1}}{N^2(1+N)^2}-\frac{3\left(-10+7N+7N^2\right)\zeta_3}{2N^2(1+N)^2}\Bigg]S_1$$
$$+\frac{\left(-2-N-N^2\right)S_2^2}{2N^2(1+N)^2}+\frac{3(N-2)(3+N)S_4}{2N^2(1+N)^2}$$
$$+\Bigg[\frac{Q_6}{N^4(1+N)^4}+\frac{2\left(4+12N-3N^3-N^4\right)S_1}{N^3(1+N)^3}-\frac{(N-1)(2+N)S_1^2}{N^2(1+N)^2}$$
$$+\frac{4S_2}{N^2(1+N)^2}\Bigg]S_{-2}+\frac{\left(2-5N-5N^2\right)S_{-2}^2}{N^2(1+N)^2}+\Bigg[\frac{\left(18+13N+13N^2\right)S_1}{2N^2(1+N)^2}$$
$$+\frac{Q_7}{2N^3(1+N)^3}\Bigg]S_{-3}-\frac{3\left(-14+N+N^2\right)S_{3,1}}{2N^2(1+N)^2}-\frac{6\left(2+3N+3N^2\right)S_{-2,2}}{N^2(1+N)^2}$$
$$+\frac{12S_{-4}}{N^2(1+N)^2}-\frac{6\left(2+3N+3N^2\right)S_{-3,1}}{N^2(1+N)^2}+\frac{12\left(2+3N+3N^2\right)S_{-2,1,1}}{N^2(1+N)^2}\Bigg\}, \tag{38}$$

[8] JB thanks S. Moch for reminding this relation.

[9] See also Ref. [111].

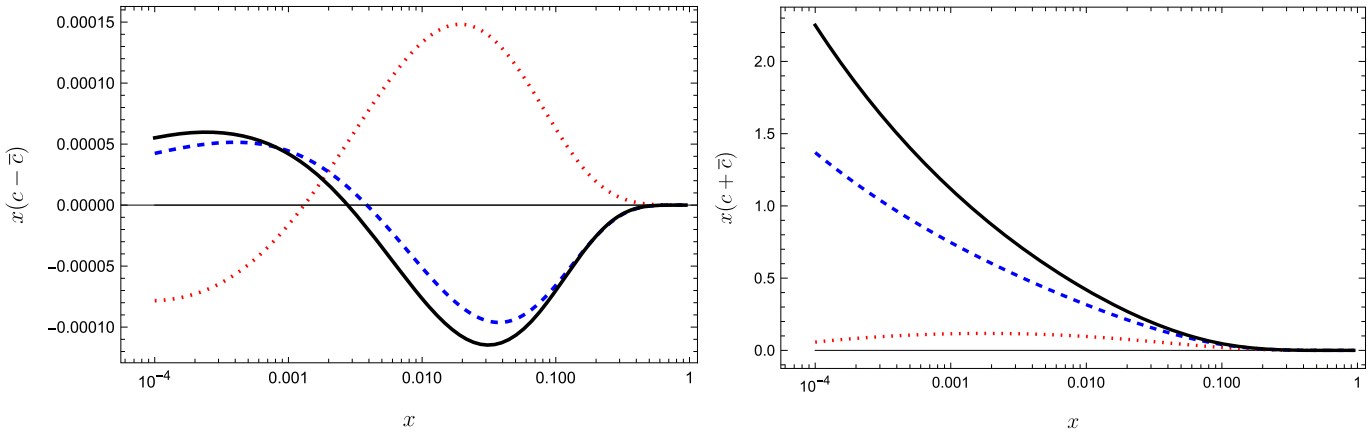

Fig. 3. The unpolarized distributions $x[c(x,Q^2)-\overline{c}(x,Q^2)]$ (left panel) and $x[c(x,Q^2)+\overline{c}(x,Q^2)]$ (right panel). Dotted lines: $Q^2 = 4$ GeV^2. Dashed lines: $Q^2 = 30$ GeV^2. Full lines: $Q^2 = 100$ GeV^2.

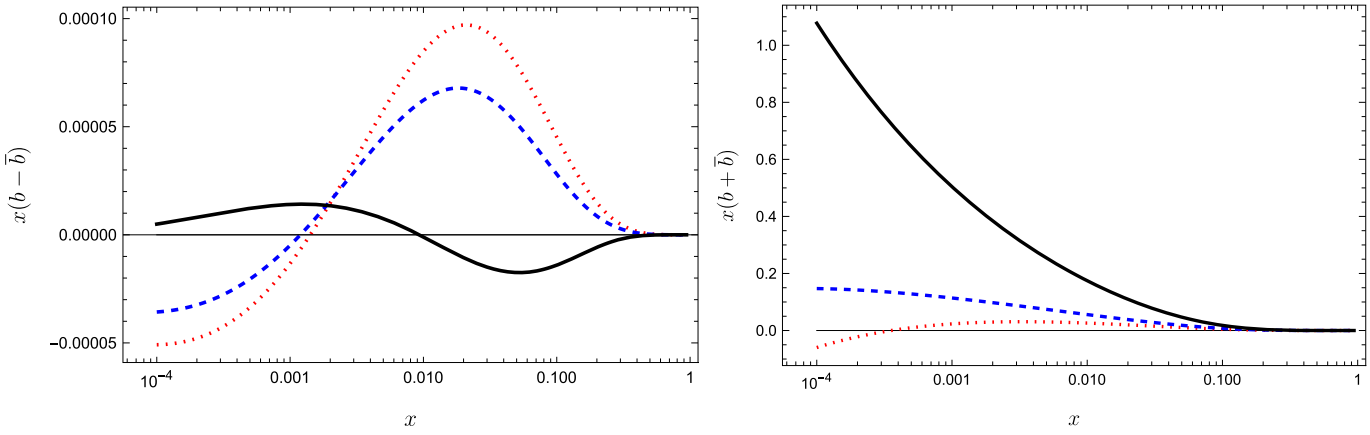

Fig. 4. The unpolarized distributions $x[b(x,Q^2)-\overline{b}(x,Q^2)]$ (left panel) and $x[b(x,Q^2)+\overline{b}(x,Q^2)]$ (right panel). Dotted lines: $Q^2 = m_b^2$. Dashed lines: $Q^2 = 30$ GeV^2. Full lines: $Q^2 = 100$ GeV^2.

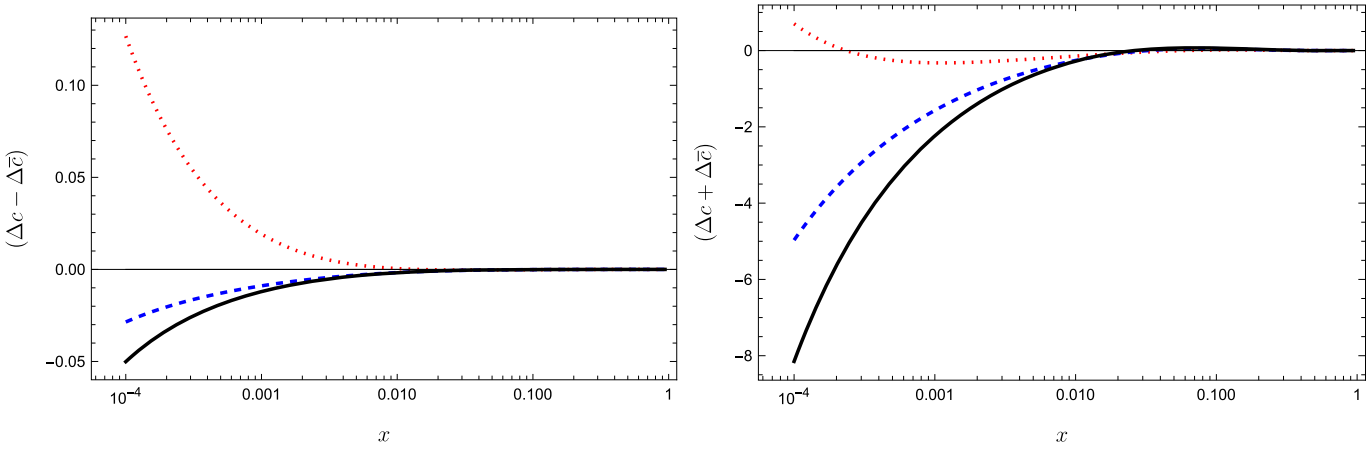

Fig. 5. The polarized distributions $[\Delta c(x,Q^2)-\Delta\overline{c}(x,Q^2)]$ (left panel) and $[\Delta c(x,Q^2)+\Delta\overline{c}(x,Q^2)]$ (right panel). Dotted lines: $Q^2 = 4$ GeV^2. Dashed lines: $Q^2 = 30$ GeV^2. Full lines: $Q^2 = 100$ GeV^2.

and the polynomials

$$Q_1 = -2N^4 - 4N^3 - 5N^2 - 3N - 2, \tag{39}$$
$$Q_2 = -6N^5 - 20N^4 - 10N^3 + N^2 - 3N - 2, \tag{40}$$
$$Q_3 = N^5 + 5N^4 - 8N^3 - 3N^2 + 3N + 6, \tag{41}$$
$$Q_4 = -3N^6 - 9N^5 - 5N^4 + 5N^3 + 19N^2 + 15N + 6, \tag{42}$$
$$Q_5 = -N^6 - N^5 + 7N^4 + 7N^3 + 19N^2 + 15N + 6, \tag{43}$$
$$Q_6 = N^6 + 7N^5 + 25N^4 + 12N^3 - 20N^2 - 31N - 10, \tag{44}$$
$$Q_7 = 6N^6 + 15N^5 - 24N^4 - 52N^3 - 39N^2 + 6N - 4, \tag{45}$$
$$Q_8 = 6N^6 + 15N^5 + 24N^4 + 12N^3 + N^2 - 18N - 4, \tag{46}$$
$$Q_9 = 15N^6 + 60N^5 + 42N^4 - 45N^3 - 37N^2 + 3N + 6, \tag{47}$$
$$Q_{10} = -16N^8 - 65N^7 - 71N^6 + 25N^5 + 58N^4 + 80N^3 + 110N^2 + 81N + 18. \tag{48}$$

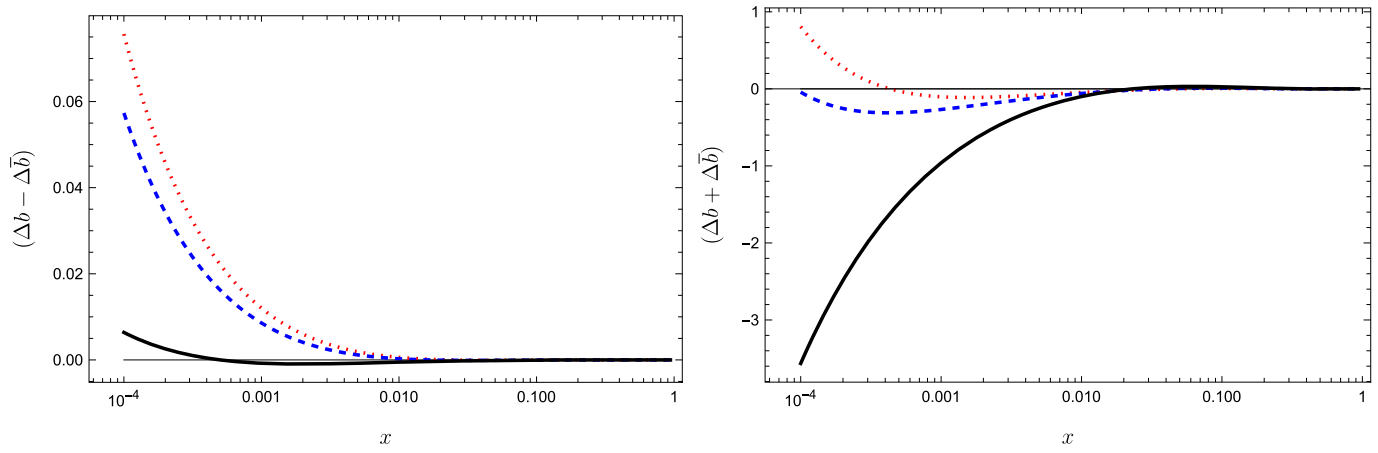

Fig. 6. The polarized distributions $[\Delta b(x,Q^2) - \Delta\bar{b}(x,Q^2)]$ (left panel) and $[\Delta b(x,Q^2) + \Delta\bar{b}(x,Q^2)]$ (right panel). Dotted lines: $Q^2 = m_b^2$. Dashed lines: $Q^2 = 30\,\mathrm{GeV}^2$. Full lines: $Q^2 = 100\,\mathrm{GeV}^2$.

The expression in x-space is given in an ancillary file. Here the first moment is non-vanishing. In the small-x region one obtains

$$\Delta a_{Qq}^{\mathrm{PS,s,(3)}}(x) \propto \frac{1}{3}\frac{d_{abc}d^{abc}}{N_c}\zeta_2 \ln(x)[(50+2\zeta_2) - 9\ln(x) - 6\ln^2(x)] \tag{49}$$

and for large-x

$$\Delta a_{Qq}^{\mathrm{PS,s,(3)}}(x) \propto \frac{1}{3}\frac{d_{abc}d^{abc}}{N_c}(1-x)\Big\{\big[14 - 4\zeta_2 - 8\zeta_3\big]\log(1-x) + \big[-3 + 2\zeta_2\big]\log^2(1-x)\Big\}. \tag{50}$$

In Fig. 2 we illustrate the constant part of the unrenormalized massive OME $\Delta\hat{A}_{Qq}^{\mathrm{PS,s,(3)}}$, $\Delta a_{Qq}^{\mathrm{PS,s,(3)}}$, as a function of x. With the OMEs calculated in this paper, the set of massive single-mass OMEs at three-loop order is now complete, extending the results reported in Refs. [47–52,112–116].

4. The heavy quark-antiquark asymmetry

Finally, we calculate the heavy quark-antiquark difference and sum distributions, $x[f_Q(x,Q^2) \mp f_{\overline{Q}}(x,Q^2)]$ and $[(\Delta)f_Q(x,Q^2) \mp (\Delta)f_{\overline{Q}}(x,Q^2)]$ by setting $\mu^2 = Q^2$, in the VFNS, for $Q = c, b$. In the unpolarized case, we refer to the parton distribution functions Ref. [117] from [118], and in the polarized case to those of Ref. [119].

For the distributions shown in Figs. 3–6, we refer to three massless flavors representing $\Sigma^{\pm}$ both for the charm and bottom distributions, Eq. (5, 6), which only differ by the logarithmic terms in the OMEs at the respective values of Q^2. The heavy-quark masses in the on-shell scheme, used in the calculation of the massive OMEs, are [63,120]

$$m_c = 1.59\ \mathrm{GeV}, \qquad m_b = 4.78\ \mathrm{GeV}. \tag{51}$$

The values of the strong coupling constant $\alpha_s(4\ \mathrm{GeV}^2) = 0.26897$, $\alpha_s(m_b^2) = 0.20452$, $\alpha_s(30\ \mathrm{GeV}^2) = 0.1972$, $\alpha_s(100\ \mathrm{GeV}^2) = 0.1706$ are consistent with the value $\alpha_s(M_Z^2) = 0.1147$. The `Fortran` programs were designed by applying code optimization [121] and we use the numerical representation of harmonic polylogarithms up to `w = 5` of Ref. [122]. Convolution integrals are calculated by the package `DAIND`, cf. Ref. [123].

In Figs. 3 to 6, we illustrate both the difference and the sum of the charm and bottom distributions, respectively, as functions of x and Q^2. Note that in the unpolarized case, the OMEs $A_{Qq}^{\mathrm{PS,(3)}}$ and $A_{Qg}^{(3)}$ have different signs, leading to partial cancellations. At the higher scales shown, the charm quark distributions are about twice bigger than those for the bottom quarks, see Figs. 3 and 4. The difference distributions $x[Q(x,Q^2) - \overline{Q}(x,Q^2)]$ take values in the range −0.0001 to +0.0015, which are oscillating since their first moments vanish.

In the polarized case, we illustrate the quark-antiquark difference distributions for the number densities in Figs. 5 and 6. Also here the charm quark distributions are about twice as large as those for bottom in the kinematic range shown, taking values between −0.05 and 0.12, more peaked towards smaller values of x. Their measurement is even more difficult, as two polarization asymmetries have to be formed. The sum distributions are widely negative in the small-x region. Correspondingly, the contributions to the nucleon momentum and spin budget by the PDF-asymmetries are very small in the heavy-quark case.

In measuring $B^-(\lambda)$ off deuteron targets, both the distributions D_8^- and Σ^- contribute in the combination $xF_3^{\gamma Z} = 1.39\,xD_8^- + 2.44\,x\Sigma^-$, and analogously in the polarized case. It turns out that in the VFNS the heavy quark-antiquark asymmetry $(\Delta)f_{Q-\overline{Q}}(x,Q^2)$ is very small but non-vanishing. An experimental measurement is challenging and will require very large luminosities and precision, despite of the fact that the heavy-flavor contributions at three-loop order are solely determined by the heavy-quark tagging part.

5. Conclusion

We calculated the massive OMEs describing the perturbative creation of the asymmetry of the heavy-quark PDFs $(\Delta)f_Q(x,Q^2) - (\Delta)f_{\overline{Q}}(x,Q^2)$ in the unpolarized and polarized cases in QCD in the variable flavor number scheme. Unlike the sum of the heavy-quark PDFs, which contribute from $O(a_s)$, their asymmetry occurs first at $O(a_s^3)$ in the VFNS. While the sum is driven by the PDFs Σ^+ and G, the difference results from Σ^-. The difference distributions contribute to the polarization asymmetry $(\Delta)B^-(\lambda)$, measured by using polarized electron and positron deep-inelastic data. It turns out that the distributions $(\Delta)f_Q(x,Q^2) - (\Delta)f_{\overline{Q}}(x,Q^2)$ are non-vanishing but very small and require huge luminosities to be measured. They contribute with a correspondingly small rate both to the nucleon momentum and nucleon spin. In the heavy-quark case, the quark and antiquark distributions are different in the VFNS.

We corrected the result for the polarized anomalous dimension $\Delta\gamma_{qq}^{\mathrm{NS,s,(2)}}$ in Refs. [46], which has been calculated by us by three different methods.

Data availability

No data was used for the research described in the article.

Declaration of competing interest

The authors declare that they have no known competing financial interests or personal relationships that could have appeared to influence the work reported in this paper.

All authors have very essentially contributed to the different part of the present work.

Acknowledgment

We thank J. Ablinger, M. Diehl, P. Marquard, P. Ploessl, and G. Salam for discussions. This work has been funded by the Austrian Science Fund (FWF) Grant DOI 10.55776/P20347. KS is supported by the European Union under the HORIZON program in Marie Skłodowska-Curie project No. 101204018 Co-funded by the European Union.

Supplementary material

Supplementary material associated with this article can be found in the online version at 10.1016/j.physletb.2026.140411

References

[1] A. Accardi, A critical appraisal and evaluation of modern PDFs, Eur. Phys. J. C 76 (8) (2016) 471 arXiv:1603.08906 [hep-ph].
[2] S. Amoroso, Snowmass 2021 whitepaper: proton structure at the precision frontier, Acta Phys. Polon. B 53 (12) (2022) 12–A13 arXiv:2203.13923 [hep-ph].
[3] J. Blümlein, H. Böttcher, QCD analysis of polarized deep inelastic scattering data, Nucl. Phys. B 841 (2010) 205–230 arXiv:1005.3113 [hep-ph].
[4] I. Borsa, M. Stratmann, W. Vogelsang, D.D. Florian, R. Sassot, Next-to-next-to-leading order global analysis of polarized parton distribution functions, Phys. Rev. Lett. 133 (15) (2024) 15 arXiv:2407.11635 [hep-ph].
[5] J. Cruz-Martinez, T. Hasenack, F. Hekhorn, G. Magni, E.R. Nocera, T.R. Rabemananjara, J. Rojo, T. Sharma, G.V. Seeventer, NNPDFpol2.0: a global determination of polarised PDFs and their uncertainties at next-to-next-to-leading order, JHEP 07 (2025) 168 arXiv:2503.11814 [hep-ph].
[6] C. Cocuzza et al. [JAM Collaboration (Spin PDF Analysis Group)], Global QCD analysis of spin PDFs in the proton with high-x and lattice constraints, Phys. Rev. D 112 (11) (2025) 114017 arXiv:2506.13616 [hep-ph].
[7] B. Lampe, E. Reya, Spin physics and polarized structure functions, Phys. Rept. 332 (2000) 1–163 arXiv:hep-ph/9810270 [hep-ph].
[8] C. Amsler et al. Review of particle physics, Phys. Lett. B 667 (2008) 1–1340. [Particle Data Group]
[9] A. Baldit et al. NA51], Study of the isospin symmetry breaking in the light quark sea of the nucleon from the Drell-Yan process, Phys. Lett. B 332 (1994) 244–250. [NA51]
[10] S. Navas, Review of particle physics, Struct. Functions 110 (2023) 2025. Phys. Rev. D. (Particle Data Group)
[11] A.I. Signal, A.W. Thomas, Possible strength of the nonperturbative strange sea of the nucleon, Phys. Lett. B 191 (1987) 205–208.
[12] M. Burkardt, B. Warr, Chiral symmetry and the charge asymmetry of the s anti-s distribution in the proton, Phys. Rev. D 45 (1992) 958–964.
[13] H. Holtmann, A. Szczurek, J. Speth, Flavor and spin of the proton and the meson cloud, Nucl. Phys. A 596 (1996) 631–669 [hep-ph/9601388].
[14] S.J. Brodsky, B.Q. Ma, The quark/anti-quark asymmetry of the nucleon sea, Phys. Lett. B 381 (1996) 317–324 [hep-ph/9604393].
[15] H.R. Christiansen, J. Magnin, Strange/anti-strange asymmetry in the nucleon sea, Phys. Lett. B 445 (1998) 8–13 ([hep-ph/9801283]) .
[16] F.G. Cao, A.I. Signal, On the phenomenological analyses of $s - \bar{s}$ asymmetry in the nucleon sea, Phys. Rev. D 60 (1999) 74021, [hep-ph/9907297].
[17] W. Melnitchouk, M. Malheiro, Strange asymmetries in the nucleon sea, Phys. Lett. B 451 (1999), 224–232 [hep-ph/9901321].
[18] V. Barone, C. Pascaud, F. Zomer, A new global analysis of DIS data and the strange sea distribution, in: A.W. Schreiber, A.G. Williams (Eds.), Contribution to the Proceedings of the Workshop on Light-Cone QCD and Nonperturbative Hadron Physics, World Scientific, 1999, pp. 167–172. [hep-ph/0004268 in Singapore].
[19] F.G. Cao, A.I. Signal, The quark anti-quark asymmetry of the strange sea of the nucleon, Phys. Lett. B 559 (2003) 229–234 [hep-ph/0302206].
[20] S. Catani, D.D. Florian, G. Rodrigo, W. Vogelsang, Perturbative generation of a strange-quark asymmetry in the nucleon, Phys. Rev. Lett. 93 (2004) 152003 [hep-ph/0404240].
[21] A. Airapetian, Quark helicity distributions in the nucleon for up, down, and strange quarks from semi-inclusive deep-inelastic scattering, Phys. Rev. D 71 (2005) 12003 [hep-ex/0407032].
[22] A. Vega, I. Schmidt, T. Gutsche, V.E. Lyubovitskij, Nonperturbative contribution to the strange-antistrange asymmetry of the nucleon sea, Phys. Rev. D 93 (5) (2016) 56001. arXiv:1511.06476 [hep-ph].
[23] M. Zhu, S. Hu, Y. Jia, Z. Mo, X. Xiong, Strange-antistrange and charm-anticharm asymmetries of pion in 't Hooft model, arxiv:2412.21152 [hep-ph].
[24] S.J. Brodsky, P. Hoyer, C. Peterson, N. Sakai, The intrinsic charm of the proton, Phys. Lett. B 93 (1980) 451–455.
[25] J. Blümlein, A kinematic condition on intrinsic charm, Phys. Lett. B 753 (2016) 619–621. arXiv:1511.00229 [hep-ph]
[26] D.J. Gross, S.B. Treiman, Light cone structure of current commutators in the gluon quark model, Phys. Rev. D 4 (1971) 1059–1072.
[27] H.D. Politzer, Asymptotic freedom: an approach to strong interactions, Phys. Rept 14 (1974) 129–180.
[28] B. Geyer, D. Robaschik, E. Wieczorek, Theory of Deep Inelastic Lepton-Hadron Scattering. 1., Fortsch. Phys. 27 (1979) 75–168.
[29] A.J. Buras, Asymptotic freedom in deep inelastic processes in the leading order and beyond, Rev. Mod. Phys. 52 (1980) 199–276.
[30] E. Reya, Perturbative Quantum Chromodynamics, Phys. Rept. 69 (1981) 195–353.
[31] J. Blümlein, The theory of deeply inelastic scattering, Prog. Part. Nucl. Phys. 69 (2013) 28–84. arXiv:1208.6087 [hep-ph].
[32] W.A. Bardeen, A.J. Buras, D.W. Duke, T. Muta, Deep inelastic scattering beyond the leading order in asymptotically free gauge theories, Phys. Rev. D 18 (1978) 3998–4017.
[33] S.A. Larin, The renormalization of the axial anomaly in dimensional regularization, Phys. Lett. B 303 (1993) 113–118 [hep-ph/9302240].
[34] M. Buza, Y. Matiounine, J. Smith, W.L.V. Neerven, Charm electroproduction viewed in the variable flavor number scheme versus fixed order perturbation theory, Eur. Phys. J. C 1(1998) 301–320 [hep-ph/9612398].
[35] M.A.G. Aivazis, J.C. Collins, F.I. Olness, W.K. Tung, Leptoproduction of heavy quarks. 2. A Unified QCD formulation of charged and neutral current processes from fixed target to collider energies, Phys. Rev. D 50 (1994) 3102–3118. arXiv:hep-ph/9312319 [hep-ph].
[36] R.S. Thorne, R.G. Roberts, A practical procedure for evolving heavy flavor structure functions, Phys. Lett. B 421 (1998) 303–311. arXiv:hep-ph/9711223 [hep-ph].
[37] J.C. Collins, Hard scattering factorization with heavy quarks: a general treatment, Phys. Rev. D 58 (1998) 94002. arXiv:hep-ph/9806259 [hep-ph].
[38] S. Forte, E. Laenen, P. Nason, J. Rojo, Heavy quarks in deep-inelastic scattering, Nucl. Phys. B 834 (2010) 116–162. arXiv:1001.2312 [hep-ph].
[39] J. Ablinger, A. Behring, J. Blümlein, A.D. Freitas, A. Manteuffel, C. Schneider, K. Schönwald, The single-mass variable flavor number scheme at three-loop order, arxiv:2510.02175 [hep-ph].
[40] M. Buza, W.L.V. Neerven, $O(\alpha_s^2)$ contributions to charm production in charged current deep inelastic Lepton-Hadron scattering, Nucl. Phys. B 500 hep-ph/9702242 (1997) 301–324.
[41] J. Blümlein, A. Hasselhuhn, T. Pfoh, The $O(\alpha_s^2)$ heavy quark corrections to charged current deep-inelastic scattering at large virtualities, Nucl. Phys. B 881 (2014) 1–41. arXiv:1401.4352 [hep-ph].
[42] J. Blümlein, N. Kochelev, On the twist-two and twist-three contributions to the spin dependent electroweak structure functions, Nucl . Phys. B 498 (1997) 285–309 [hep-ph/9612318].
[43] S. Moch, J.A.M. Vermaseren, A. Vogt, The three loop splitting functions in QCD: the nonsinglet case, Nucl. Phys. B 688 (2004) 101–134 [hep-ph/0403192].
[44] S. Moch, J.A.M. Vermaseren, A. Vogt, On γ_5 in higher-order QCD calculations and the NNLO evolution of the polarized valence distribution, Phys. Lett. B 748 (2015) 432–438. arXiv:1506.04517 [hep-ph].
[45] J. Blümlein, P. Marquard, C. Schneider, K. Schönwald, The three-loop unpolarized and polarized non-singlet anomalous dimensions from off shell operator matrix elements, Nucl. Phys. B 971 (2021) 115542. arXiv:2107.06267 [hep-ph].
[46] J. Blümlein, P. Marquard, C. Schneider, K. Schönwald, The three-loop polarized singlet anomalous dimensions from off-shell operator matrix elements, JHEP 01 (2022) 193. and Erratum arXiv:2111.12401 [hep-ph].
[47] J. Ablinger, A. Behring, J. Blümlein, A.D. Freitas, A. Manteuffel, C. Schneider, The 3-loop pure singlet heavy flavor contributions to the structure function $F_2(x, Q^2)$ and the anomalous dimension, Nucl. Phys. B 890 (2014) 48–151. arXiv:1409.1135 [hep-ph].
[48] J. Ablinger, A. Behring, J. Blümlein, A.D. Freitas, A. Manteuffel, C. Schneider, K. Schönwald, The three-loop single mass polarized pure singlet operator matrix element, Nucl. Phys. B 953 (2020) 114945. arXiv:1912.02536 [hep-ph].
[49] J. Ablinger, A. Behring, J. Blümlein, A.D. Freitas, A. Manteuffel, C. Schneider, K. Schönwald, The first-order factorizable contributions to the three-loop massive operator matrix elements $A_{Qg}^{(3)}$ and $\Delta A_{Qg}^{(3)}$, Nucl. Phys. B 999 (2024) 116427. arXiv:2311.00644 [hep-ph].
[50] J. Ablinger, A. Behring, J. Blümlein, A.D. Freitas, A. Manteuffel, C. Schneider, K. Schönwald, The non-first-order-factorizable contributions to the three-loop single-mass operator matrix elements $A_{Qg}^{(3)}$ and $\Delta A_{Qg}^{(3)}$, Phys. Lett. B 854 (2024) 138713. arXiv:2403.00513 [hep-ph].
[51] A. Behring, I. Bierenbaum, J. Blümlein, A.D. Freitas, S. Klein, F.W. brock, The logarithmic contributions to the $O(\alpha_s^3)$ asymptotic massive Wilson coefficients and operator matrix elements in deeply inelastic scattering, Eur. Phys. J. C 74 (9) (2014) 3033. arXiv:1403.6356 [hep-ph].
[52] J. Ablinger, A. Behring, J. Blümlein, A.D. Freitas, A. Hasselhuhn, A. Manteuffel, M. Round, C. Schneider, F.W. brock, The 3-loop non-singlet heavy flavor contributions and anomalous dimensions for the structure function $F_2(x, Q^2)$ and transversity, Nucl. Phys. B 886 (2014) 733–823. arXiv:1406.4654 [hep-ph].
[53] E. Derman, Tests for a weak neutral current in $l^{\pm}n \to l^{\pm} + anything$ at high energy, Phys. Rev. D 7 (1973) 2755–2775.
[54] J. Blümlein, M. Klein, T. Naumann, T. Riemann, Structure Functions, Quark Distributions and Λ_{QCD} at HERA, Proc. of the HERA Workshop, I of *Hamburg*, 1987.
[55] D.Y. Bardin, J. Blümlein, P. Christova, L. Kalinovskaya, $O(\alpha)$ QED corrections to neutral current polarized deep-inelastic lepton-nucleon scattering, Nucl. Phys. B 506 (1997) 295–328 hep-ph/9612435.
[56] A. Argento, Measurement of the interference structure function $xG_3(x)$ in muon-nucleon scattering, Phys. Lett. B 140 (1984) 142–144.
[57] H. Abramowicz, Combination of measurements of inclusive deep inelastic $e^{\pm}p$ scattering cross sections and QCD analysis of HERA data, Eur. Phys. J. C 75 (12) (2015) 580. arXiv:1506.06042 [hep-ex].

[58] D. Boer, Gluons and the quark sea at high energies: distributions, polarization, tomography, arxiv:1108.1713 [Nucl-th].
[59] W. Melnitchouk, Jlab, EW physics with positrons at the EIC, talk May 6th 2020. Y. Furletova, EIC positron working group, talk, With the positron beam at EIC.
[60] J.L. Fernandez, A large hadron electron collider at CERN: report on the physics and design concepts for machine and detector, J. Phys. G 39 (2012) 75001. Physics, arXiv:1206.2913 [acc-ph].
[61] P. Agostini, The large HadronElectron collider at the HL-LHC, J. Phys. G 48 (11) (2021) 110501. LHeC and FCC-he Study Group., arXiv:2007.14491. [hep-ex]
[62] I. Bierenbaum, J. Blümlein, S. Klein, Mellin moments of the $O(\alpha_s^3)$ heavy flavor contributions to unpolarized deep-inelastic scattering at $Q^2 \gg m^2$ and anomalous dimensions, Nucl. Phys. B 820 (2009) 417–482. arXiv:0904.3563 [hep-ph].
[63] K.A. Olive, et al. Particle Data Group, Review of particle physics Chin. Phys. 38 (2014) 090001.
[64] P. Nogueira, Automatic Feynman graph generation, J. Comput. Phys. 105 (1993) 279–289.
[65] J.A.M. Vermaseren, New Features of FORM, math-ph/0010025,
[66] M. Tentyukov, J.A.M. Vermaseren, The multithreaded version of FORM, Comput. Phys. Commun. 181 hep-ph/0702279 (2010) 1419–1427.
[67] T.V. Ritbergen, A.N. Schellekens, J.A.M. Vermaseren, Group theory factors for Feynman diagrams, Int. J. Mod. Phys. A 14 hep-ph/9802376 (1999) 41–96.
[68] C. Studerus, Reduze-Feynman integral reduction in C, Comput. Phys. Commun. (2010) 1293–1300. Physics, arXiv:0912.2546 [comp-ph].
[69] A. Manteuffel, C. Studerus, Technical Report, Reduze 2 - Distributed Feynman Integral Reduction, arXiv:1201.4330 [hep-ph].
[70] J. Blümlein, C. Schneider, Analytic computing methods for precision calculations in quantum field theory, Int. J. Mod. Phys. A 33 (17) (2018) 1830015. arXiv:1809.02889 [hep-ph].
[71] J. Blümlein, C. Schneider, The SAGEX review on scattering amplitudes chapter 4: multi-loop Feynman integrals, J. Phys. A 55 (44) (2022) 443005. arXiv:2203.13015 [hep-th].
[72] M. Karr, Summation in finite terms, J. ACM 28 (1981) 305–350.
[73] M. Bronstein, On solutions of linear ordinary difference equations in their coefficient field, J. Symbolic Comput. 29 (6) (2000) 841–877.
[74] C. Schneider, Technical Report, Johannes Kepler University, 2001.
[75] C. Schneider, A collection of denominator bounds to solve parameterized linear difference equations in ΠΣ-extensions, An Univ. Timisoara Ser. Mat.-Inf. 42 (2004) 163–179.
[76] C. Schneider, Solving parameterized linear difference equations in terms of indefinite nested sums and products, J. Differ. Equations Appl. 11 (2005) 799–821.
[77] C. Schneider, Degree bounds to find polynomial solutions of parameterized linear difference equations in ΠΣ-fields, Appl. Algebra Eng. Comm. Comput. 16 (1) (2005) 1–32.
[78] C. Schneider, Simplifying sums in ΠΣ*-extensions, J. Algebra Appl. 6 (2007) 415–441.
[79] C. Schneider, A symbolic summation approach to find optimal nested sum representations, Clay Math. Proc. 12 (2010) 285–308. arXiv:0904.2323 [Cs.SC].
[80] C. Schneider, Parameterized telescoping proves algebraic independence of sums, Ann. Comb. 14 (2010) 533–552. arXiv:0808.2596 [Cs.SC].
[81] C. Schneider, Fast algorithms for refined parameterized telescoping in difference fields, computer algebra and polynomials, applications of algebra and number theory, Lect. Not. Comput. Sci. 8942 (2015) 157–191. arXiv:1307.7887 [Cs.SC].
[82] C. Schneider, A difference ring theory for symbolic summation, J. Symb. Comput. 72 (2016) 82–127. arXiv:1408.2776 [Cs.SC].
[83] C. Schneider, Summation theory II: characterizations of $R\Pi\Sigma^*$-extensions and algorithmic aspects, J. Symb. Comput. 80 (2017) 616–664. arXiv:1603.04285 [Cs.SC].
[84] S.A. Abramov, M. Bronstein, M. Petkovšek, C. Schneider, On rational and hypergeometric solutions of linear ordinary difference equations in $\Pi\Sigma^*$-field extensions, J. Symb. Comput. 107 (2021) 23–66. arXiv:2005.04944 [Cs.SC].
[85] S.A. Abramov, M. Petkovšek, D'Alembertian solutions of linear differential and difference equations, in: J. Gathen (Ed.), Proceedings of ISSAC'94, ISSAC'94New York, ACM Press, 1994, pp. 169–174.
[86] C. Schneider, Symbolic summation assists combinatorics, Sém. Lothar. Combin. 56 (2007) 1–36. Article B56b.
[87] C. Schneider, Simplifying Multiple Sums in Difference Fields, in: Computer Algebra in Quantum Field Theory: Integration, Summation and Special Functions Texts and Monographs in Symbolic Computation eds, Springer, Wien, arxiv:1304.4134 [Cs.SC]. 2013.
[88] J.A.M. Vermaseren, Harmonic sums, Mellin transforms and integrals, Int. J. Mod. Phys. A 14 hep-ph/9806280 (1999) 2037–2076.
[89] J. Blümlein, S. Kurth, Harmonic sums and Mellin transforms up to two loop order, Phys. Rev. D 60 hep-ph/9810241 (1999) 14018.
[90] J. Ablinger, J. Blümlein, C. Schneider, Analytic and algorithmic aspects of generalized harmonic sums and polylogarithms, J. Math. Phys. 54 (2013) 82301. arXiv:1302.0378 [Math-ph].
[91] J. Ablinger, J. Blümlein, C. Schneider, Harmonic sums and polylogarithms generated by cyclotomic polynomials, J. Math. Phys. 52 (2011) 102301. arXiv:1105.6063 [Math-ph].
[92] J. Ablinger, J. Blümlein, C.G. Raab, C. Schneider, Iterated binomial sums and their associated iterated integrals, J. Math. Phys. 55 (2014) 112301. arXiv:1407.1822 [hep-th].
[93] E. Remiddi, J.A.M. Vermaseren, Harmonic polylogarithms, Int. J. Mod. Phys. A 15 (2000) 725–754 (hep-ph/9905237).
[94] J. Blümlein, Algebraic relations between harmonic sums and associated quantities, Comput. Phys. Commun. 159 (hep-ph/0311046) (2004) 19–54.
[95] J. Blümlein, Structural relations of harmonic sums and Mellin transforms up to weight w = 5, Comput. Phys. Commun. 180 (2009) 2218–2249. arXiv:0901.3106 [hep-ph].
[96] J. Blümlein, D.J. Broadhurst, J.A.M. Vermaseren, The multiple zeta value data mine, Comput. Phys. Commun. 181 (2010) 582–625. arXiv:0907.2557 [Math-ph].
[97] J. Ablinger, A Computer Algebra Toolbox for Harmonic Sums Related to Particle Physics, Technical Report, JKU Linz, 2009. arXiv:1011.1176 [Math-ph].
[98] J. Ablinger, Computer Algebra Algorithms for Special Functions in Particle Physics, Technical Report, Ph.D. Thesis, 2012. arXiv:1305.0687 [Math-ph].
[99] J. Ablinger, The package HarmonicSums: computer algebra and analytic aspects of nested sums, PoS in: LL2014), , p. 19. arXiv:1407.6180 [Cs.SC].
[100] J. Ablinger, Discovering and proving infinite binomial sums identities, Exper. Math. 26 (1) (2016) 62–71. arXiv:1507.01703 [Math.NT].
[101] J. Ablinger, Inverse Mellin transform of holonomic sequences, PoS 2016. LL2016. 67
[102] J. Ablinger, An improved method to compute the inverse Mellin transform of holonomic sequences, PoS 2018, LL2018 p. 063.
[103] J. Ablinger, in: Computing the inverse Mellin transform of holonomic sequences using Kovacic's algorithm, PoS (RADCOR2017) 2017, p. 1. arXiv:1801.01039 [Cs.SC].
[104] J. Ablinger, Discovering and proving infinite pochhammer sum identities, arxiv:1902.11001 [Math.CO].
[105] J. Ablinger, J. Blümlein, C. Schneider, Iterated integrals over letters induced by quadratic forms, Phys. Rev. D 103 (9) (2021) 96025. arXiv:2103.08330 [hep-ph].
[106] L. Bonino, T. Gehrmann, M. Löchner, K. Schönwald, G. Stagnitto, Polarized neutral and charged current semi-inclusive deep-inelastic scattering at NNLO in QCD, arxiv:2510.00100 [hep-ph].
[107] A. Behring, J. Blümlein, A.D. Freitas, A. Goedicke, S. Klein, A. Manteuffel, C. Schneider, K. Schönwald, The polarized three-loop anomalous dimensions from on-shell massive operator matrix elements, Nucl. Phys. B 948 (2019) 114753. arXiv:1908.03779 [hep-ph].
[108] Y.J. Zhu, The N^{3}PLXLO twist-2 matching of helicity TMDs and SIDIS q_* spectrum, arxiv:2509.01655v3 [hep-ph].
[109] Y. Matiounine, J. Smith, W.L.V. Neerven, Two loop operator matrix elements calculated up to finite terms, Phys. Rev. D 57 (1998) 6701–6722. arXiv:hep-ph/9801224 [hep-ph].
[110] J. Blumlein, V. Ravindran, W.L.V. Neerven, Nucl. Phys. B 586 (2000) 349–381. arXiv:hep-ph/0004172 [hep-ph].
[111] J. Blümlein, P. Marquard, C. Schneider, K. Schönwald, The two-loop massless off-shell QCD operator matrix elements to finite terms, Nucl. Phys. B 980 (2022) 115794. arXiv:2202.03216 [hep-ph].
[112] J. Ablinger, J. Blümlein, S. Klein, C. Schneider, F.W. brock, The $O(\alpha_s^3)$ massive operator matrix elements of $O(N_F)$ for the structure function $F_2(x, Q^2)$ and transversity, Nucl. Phys. B 844 (2011) 26–54. arXiv:1008.3347 [hep-ph].
[113] J. Ablinger, J. Blümlein, A.D. Freitas, A. Hasselhuhn, A. Manteuffel, M. Round, C. Schneider, F.W. brock, The transition matrix element $A_{gq}(N)$ of the variable flavor number scheme at $O(\alpha_s^3)$, Nucl. Phys. B 882 (2014) 263–288. arXiv:1402.0359 [hep-ph].
[114] J. Ablinger, A. Behring, J. Blümlein, A.D. Freitas, A. Goedicke, A. Manteuffel, C. Schneider, K. Schönwald, The unpolarized and polarized single-mass three-loop heavy flavor operator matrix elements $A_{gg,Q}$ and $\Delta A_{gg,Q}$, JHEP 12 (2022) 134. arXiv:2211.05462 [hep-ph].
[115] J. Blümlein, A.D. Freitas, M. Saragnese, C. Schneider, K. Schönwald, Logarithmic contributions to the polarized $O(\alpha_s^3)$ asymptotic massive Wilson coefficients and operator matrix elements in deeply inelastic scattering, Phys. Rev. D 104 (3) (2021) 34030. arXiv:2105.09572 [hep-ph].
[116] A. Behring, J. Blümlein, A.D. Freitas, A. Manteuffel, K. Schönwald, C. Schneider, The polarized transition matrix element $A_{gq}(N)$ of the variable flavor number scheme at $O(\alpha_s^3)$, Nucl. Phys. B 964 (2021) 115331. arXiv:2101.05733 [hep-ph].
[117] S. Alekhin, J. Blümlein, S. Moch, R. Placakyte, Parton distribution functions, α_s, and heavy-quark masses for LHC Run II, Phys. Rev. D 96 (1) (2017) 14011. arXiv:1701.05838 [hep-ph].
[118] A. Buckley, et al., LHAPDF6: parton density access in the LHC precision era, Eur. Phys. J. C 75 (2015) 132. arXiv:1412.7420 [hep-ph].
[119] J. Blümlein, M. Saragnese, Next-to-next-to-leading order evolution of polarized parton densities in the Larin scheme, Phys. Rev. D 110 (3) (2024) 34006. arXiv:2405.17252 [hep-ph].
[120] S. Alekhin, J. Blümlein, K. Daum, K. Lipka, S. Moch, Precise charm-quark mass from deep-inelastic scattering, Phys. Lett. B 720 (2013) 172–176. arXiv:1212.2355 [Hep-ph].
[121] B. Ruijl, T. Ueda, J. Vermaseren, FORM version 4.2, arxiv:1707.06453 [hep-ph] edition.
[122] T. Gehrmann, E. Remiddi, Numerical evaluation of harmonic polylogarithms, Comput. Phys. Commun. 141 (2001) 296–312 [hep-ph/0107173].
[123] R. Piessens, An algorithm for automatic integration, Angew. Informatik 9 (1973) 399–401.